J Clin Periodontol 2014; 41: 172–180 doi: 10.1111/jcpe.12187

Journal of Clinical Periodontology

Improving oral implant osseointegration in a murine model via Wnt signal amplification

Sylvain Mouraret[1,2], Daniel J. Hunter[1], Claire Bardet[1,3], Antoine Popelut[2], John B. Brunski[1], Catherine Chaussain[3], Philippe Bouchard[2] and Jill A. Helms[1]

[1]Division of Plastic and Reconstructive Surgery, Department of Surgery, Stanford School of Medicine, Stanford, CA, USA; [2]Department of Periodontology, Service of Odontology, Rothschild Hospital, AP-HP, Paris 7 – Denis, Diderot University, U.F.R. of Odontology, Paris, France; [3]Dental School University Paris Descartes PRES Sorbonne Paris Cité, Montrouge, France

Mouraret S, Hunter DJ, Bardet C, Popelut A, Brunski JB, Chaussain C, Bouchard P, Helms JA. Improving oral implant osseointegration in a murine model via Wnt signal amplification. J Clin Periodontol 2014; 41: 172–180. doi: 10.1111/jcpe.12187.

Abstract

Aim: To determine the key biological events occurring during implant failure and then we use this knowledge to develop new biology-based strategies that improve osseointegration.

Materials and Methods: Wild-type and $Axin2^{LacZ/LacZ}$ adult male mice underwent oral implant placement, with and without primary stability. Peri-implant tissues were evaluated using histology, alkaline phosphatase (ALP) activity, tartrate resistant acid phosphatase (TRAP) activity and TUNEL staining. In addition, mineralization sites, collagenous matrix organization and the expression of bone markers in the peri-implant tissues were assessed.

Results: Maxillary implants lacking primary stability show histological evidence of persistent fibrous encapsulation and mobility, which recapitulates the clinical problems of implant failure. Despite histological and molecular evidence of fibrous encapsulation, osteoblasts in the gap interface exhibit robust ALP activity. This mineralization activity is counteracted by osteoclast activity that resorbs any new bony matrix and consequently, the fibrous encapsulation remains. Using a genetic mouse model, we show that implants lacking primary stability undergo osseointegration, provided that Wnt signalling is amplified.

Conclusions: In a mouse model of oral implant failure caused by a lack of primary stability, we find evidence of active mineralization. This mineralization, however, is outpaced by robust bone resorption, which culminates in persistent fibrous encapsulation of the implant. Fibrous encapsulation can be prevented and osseointegration assured if Wnt signalling is elevated at the time of implant placement.

Key words: Axin2; bone; dental; fibrointegration; fibrous encapsulation; histology; *in vivo*; maxilla; mice; model; oral cavity; Wnt

Accepted for publication 29 September 2013

Conflict of interest and source of funding statement

The authors declare that they have no conflict of interest. This study was supported by a grant to J.A.H. from the California Institute of Regenerative Medicine (CIRM) TR1-01249.

Osseointegration is deemed a requirement for the clinical success of an implant (Branemark et al. 1977), but accurately assessing the extent of osseointegration can oftentimes be problematic. Osseointegration is defined as a direct anchorage of the implant to surrounding bone under functional loading, and simple methods to assess this status include radiographs and torque wrenches (Albrektsson et al. 1986). More complex methods include devices that use vibrational frequency to measure implant stability (Meredith et al. 1996), but these have inconsistent

results (Huwiler et al. 2007). Thus, clinicians are often left with obscure criteria by which to determine whether osseointegration has been achieved.

Although not explicitly stated, there is a long-standing assumption that implants require primary stability in order to osseointegrate (Meredith 1998). The clinical literature, however, provides examples of implants that exhibit primary stability at the time of placement but then transiently lose this stability only to regain it at some later time-point (reviewed in Raghavendra et al. 2005). The biology underlying this seemingly contradictory sequence of events is unknown.

In previous studies, we directly tested the assumption that primary stability is required for osseointegration by creating a gap interface between an implant and the surrounding cortex bone (Leucht et al. 2007, Wazen et al. 2013). A gap-type interface necessarily creates an environment in which the implant lacks primary stability and thus provided us with an experimental model in which to assess implant failure. We found, however, that when a gap-type interface was created in the tibia, osseointegration still occurred, without any apparent intermediate step of fibrous encapsulation, provided the implant was stabilized (Leucht et al. 2007, 2012, Wazen et al. 2013). There are, however, notable differences between long bones and craniofacial bones including embryonic origins (Leucht et al. 2008a), their osteogenic plasticity (Leucht et al. 2008a, Richardson 2009), and in the presence (or absence) of an osteogenic marrow cavity. We began this project with the objective of understanding biological criteria of successful oral implant osseointegration, using a murine maxillary model rather than a tibial model. We then explored the possibility of preventing implant failure by creating an environment of elevated Wnt signalling around the implant. We specifically employed Wnt reporter ($Axin2^{LacZ/LacZ}$) mice for this purpose because of they represent a robust model of enhanced Wnt signalling (Minear et al. 2010, Liu et al. 2013). In doing so, we gained new insights into the biology of fibrous encapsulation and the tantilizing possibility that this end-stage failure state may be reversible.

Materials and Methods

Animal husbandry

All procedures were approved by the Stanford Committee on Animal Research. Wild-type and $Axin2^{LacZ/LacZ}$ skeletally mature male mice weighing an average of 28 g were obtained from the Jackson Laboratory (Bar Harbor, ME). Animals were given a soft diet food (Bio Serv product #S3472) and water *ad libitum*. No antibiotics were given to the operated animals and there was no evidence of infection or prolonged inflammation at the surgical site.

Implant surgery

Forty adult mice wild type and ten $Axin2^{LacZ/LacZ}$ mice (males, 3–5 months old) were anaesthetized with an intraperitoneal injection of Ketamine (80 mg/kg) and Xylazine (16 mg/kg). The mouth was rinsed using a povidone-iodine solution for 1 min followed by a sulcular incision that extended from the maxillary first molar to the mid-point on the alveolar crest. A full-thickness flap was elevated; a pilot hole was made to prepare the implant bed on the crest 1.5 mm in front of the first maxillary molar, using a Ø 0.3 mm pilot drill bit (Drill Bit City, Chicago, IL, USA). Then animals were divided into two groups, those in which the implant had primary stability (24) and those in which primary stability was lacking (17), see Table 1. For the former cases, the pilot drill hole was followed with a drill bit of Ø 0.45 mm, using a low-speed dental engine (800 rpm). The surgical site was carefully rinsed and the titanium implant (0.6 mm diameter titanium-6 Aluminium-4 Vanadium alloy "Retopins"; NTI Kahla GmbH, Kahla, Germany) was cut at length of 2 mm and was inserted in the bed preparation.

In cases where the implant lacked primary stability, the pilot drill hole was followed with a drill bit up to a final size of Ø 0.65 mm into which a 0.6 mm implant was placed. The larger hole ensured that the implant lacked primary stability at the time of placement.

The flap was closed using non-absorbable single interrupted sutures (Ethilon monofilament 9-0, Johnson & Johnson Medical, Piscataway, NJ, USA). Following surgery, mice received subcutaneous injections of buprenorphine (0.05–0.1 mg/kg) for analgesia once a day for 3 days. Mice were killed at 7, 14, 21 and 28 days post-surgery.

Sample preparation, processing, histology

Maxillae were harvested, the skin and outer layers of muscle were removed and the tissues fixed and processed as described (Mouraret et al. 2013). Histological stains, Movat's pentachrome, Aniline blue and Picrosirius red were preformed.

Cellular assays

Alkaline phosphatase (ALP) activity and tartrate-resistant acid phosphatase (TRAP) activity were performed using standard procedures (Mouraret et al. 2013). After developing, the slides were dehydrated in a series of ethanol and xylene and subsequently cover-slipped with Permount mounting media.

Immunohistochemistry

Immunostaining was performed using standard procedures (Mouraret et al. 2013). Antibodies used include proliferating cell nuclear antigen (PCNA, Invitrogen kit, Camarillo, CA, USA, 1/2000), Osteocalcin (Abcam ab93876, Cambridge, MA,

Table 1. Design features of implants

Implant type	Genotype	Number of implants post-surgery			
		Day 7	Day 14	Day 21	Day 28
Direct contact	CD1 wild type	6	6	6	6
Gap interface	CD1 wild type	3	7	4	3
Gap interface	$Axin2^{LacZ/LacZ}$	2	3	4	1

USA, 1/2000), Osteopontin (NIH LF 175, Bethesday, MD, USA, 1/4000), Decorin (NIH LF 113, 1/1000) and Fibromodulin (LF 149, 1/2000). Negative controls were performed during each experiment. Only when there was no evidence of staining were the results considered informative and included in the manuscript.

Histomorphometric analyses

Maxillae were collected on post-surgical day 21 to quantify the bone-implant contact for the direct contact, gap interface, and $Axin2^{LacZ/LacZ}$ mice. The 0.6 mm implant was represented across 20 tissue sections; at least four sections were used to quantify the bone-implant contact. All sections were stained with Aniline blue, which labels osteoid matrix. The sections were photographed using a Leica digital imaging system at the same magnification. The resulting digital images were analysed with Adobe Photoshop CS5. The ruler tool was used to make all measurements. For each section, the length along the implant surface that was directly contacting the bone was determined for both the surfaces. Then, the actual surface length along each of the two sides was measured. Implants were fabricated from titanium and thus had to be removed prior to tissue sectioning. Therefore, the void left by the implant was designated as the implant surface. We defined bone-implant contact (BIC) as the lack of intervening soft tissue between histological bone and this void where the implant had resided. The percentage of BIC was then calculated for both sides of the implant on each of the sections obtained from each implant, using the BIC length as the numerator and the measured implant length of the implant as the denominator.

Statistical analyses

Results are presented as the mean ± SEM. Student's *t*-test was used to quantify differences described in this article. The $p \leq 0.05$ was considered significant.

Results

Osseointegration occurs by post-surgery day 14 in a mouse oral implant model

Our objective at the outset was to recapitulate a condition of oral implant osseointegration (i.e. direct bone-implant contact) and in doing so, capture the limitations and issues that confront clinicians. An implant was placed immediately anterior to the first maxillary molar, along the alveolar crest in the edentulous space (Fig. S1).

Histological analyses showed that on post-surgery day 7 evidence of bone formation was detectable in the peri-implant space (Fig. 1a). The new bone appeared to extend from the periosteal surfaces of the native maxillary bone (Fig. 1a′,a″). On day 14, more new bone apparently arising from the periosteum was in contact with the implant surface (Fig. 1b–b″), indicating that the implant was osseointegrated at this point. The maximum amount of bone in contact with the implant surface was achieved by day 21 (Fig. 1c–c″). At day 28, the bone continued to mature and developed a more lamellar organization (Fig. 1d–d″). Of 24 implants placed with this direct bone-implant contact, 23 exhibited primary stability (96%), on par with what is reported for oral implant osseointegration in humans (Pjetursson et al. 2012). By histological assessment, 17 achieved osseointegration (74%).

Murine peri-implant tissue responses are similar to large animal responses

In a separate paper, we describe the peri-implant tissue reaction to the maxillary surgery, and the molecular and cellular mechanisms underlying oral implant osseointegration in this

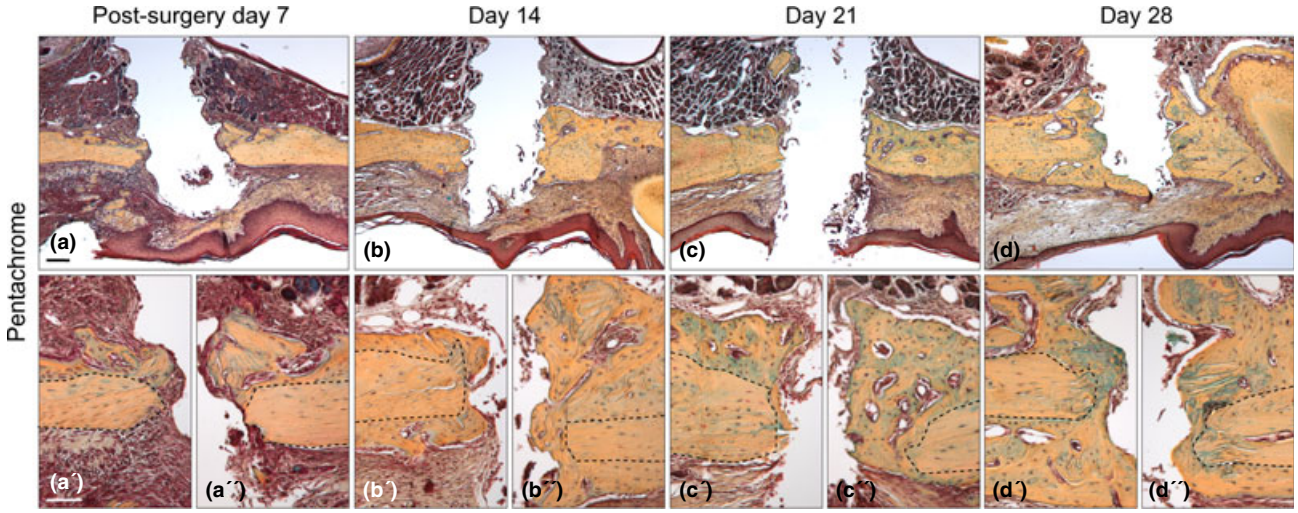

Fig. 1. Chronology of implant osseointegration in the oral cavity. (a) Representative sagittal tissue section through a maxilla implant site on post-surgery day 7, stained with Pentachrome. The yellow/blue colour denotes collagen-rich matrix in the defect site. (a′ and a″) High magnification images of the bone in contact with the implant; black dotted lines outline original bone. (b) Maxilla implant site on post-surgery day 14. (b′ and b″) High magnification image of the bone in contact with the implant. (c) Representative sagittal tissue section through a maxillary implant. (c′ and c″) High magnification images on post-surgery day 21. (d) Representative sagittal tissue section through a maxillary implant site on post-surgery day 28, stained with Pentachrome. (d′ and d″) High magnification image of the bone in contact with the implant. Scale bars: (a–d), 200 μm; (a′–d′) 50 μm.

model (Mouraret et al. 2013). Here, we focused on differences between implants that had a direct contact with the maxillary bone (i.e. those that had primary stability; Fig. 2a) and those implants that had a gap-type interface and consequently lacked primary stability (Fig. 2b). Even after 28 days, implants placed in gap-type interfaces remained surrounded by fibrous connective tissue with no evidence of osseointegration (Fig. 2c).

Bone formation was not curtailed around implants that lacked primary stability. In addition to the native maxillary cortical bone (dotted white line, Fig. 2d), aniline blue staining identified the newly mineralized matrix induced by implant bed preparation (Mouraret et al. 2013) (arrow, Fig. 2d). Despite this robust bone formation, a fibrous, non-mineralized tissue still occupied the peri-implant space (arrow, Fig. 2d). Using Picrosirus red staining and polarized light (Dayan et al. 1989), the collagenous matrix in the new bone was evident (arrow, Fig. 2e) as was the persistent lack of an organized collagenous matrix in the gap interface (Fig. 2e). Most of the fibrous tissue encapsulating the implant was immunopositive for Decorin (Weis et al. 2005), an proteoglycan involved in connective tissue matrix assembly (Fig. 2f).

Molecular differences between osseointegration and fibrous encapsulation

Around implants lacking primary stability we detected no appreciable change in the organization of the peri-implant tissues between days 7 and 28, suggesting that fibrous encapsulation represented some end-stage process of cell differentiation (Figs 1 and 2). To determine if this indeed was the case we evaluated the peri-implant tissues for evidence of bone turnover. Our controls were the primary stability cases, where a direct contact between bone and the implant existed. In these direct-contact cases, alkaline phosphatase (ALP) activity (Stucki et al. 2001) marked sites of active bone mineralization around the implant (arrows Fig. 3a). ALP activity was specifically located to sites of new bone deposition, outlining the lacunae and periosteal surfaces where active mineralization was taking place (Fig. 3a).

Around implants lacking primary stability (e.g. gap-interface cases), ALP activity was evident around the new bone (red arrow, Fig. 3b) but was conspicuously absent in the 125 micron-wide zone of fibrous tissue immediately adjacent to the implant (blue arrow, Fig. 3b). A thin zone of ALP activity was consistently observed in a 50 micron wide zone adjacent to the native maxillary bone (yellow arrow, Fig. 3b). Thus, bone formation and ALP activity were consistent features in the tissues around implants that lacked primary stability, but their distribution was absent from the peri-implant tissues.

What repressed ALP activity and consequently, new bone formation in the zone immediately adjacent to the

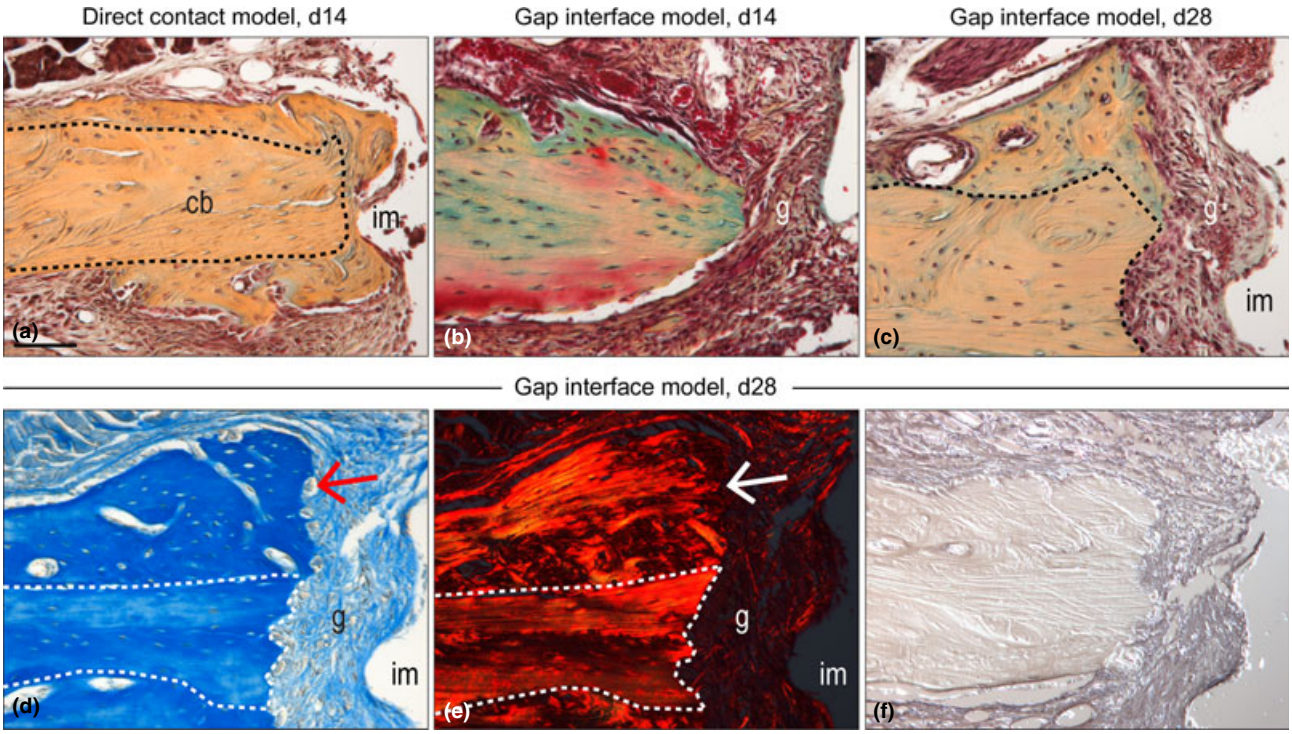

Fig. 2. Comparative histology of osseointegrated and failed oral implants. (a) Representative tissue section through a direct contact model maxilla implant site on post-surgery day 14, stained with Pentachrome; black-dotted line indicates native bone. The yellow/blue colour denotes collagen-rich matrix. (b) Gap interface implant model on post-surgery day 14 and (c) day 28 stained with Pentachrome. (d) Aniline blue staining of maxillary gap interface implant model on post-surgery day 28, the red arrow denotes new bone formation. (e) Picrosirius Red staining of maxillary gap interface implant model on post-surgery day 28, observed with polarized light; the white arrow denotes the orientation of the new collagen. (f) Representative tissue section through a gap interface implant model on post-surgery day 28, immunostained for Decorin. Scale bars: (a–d), 100 μm.

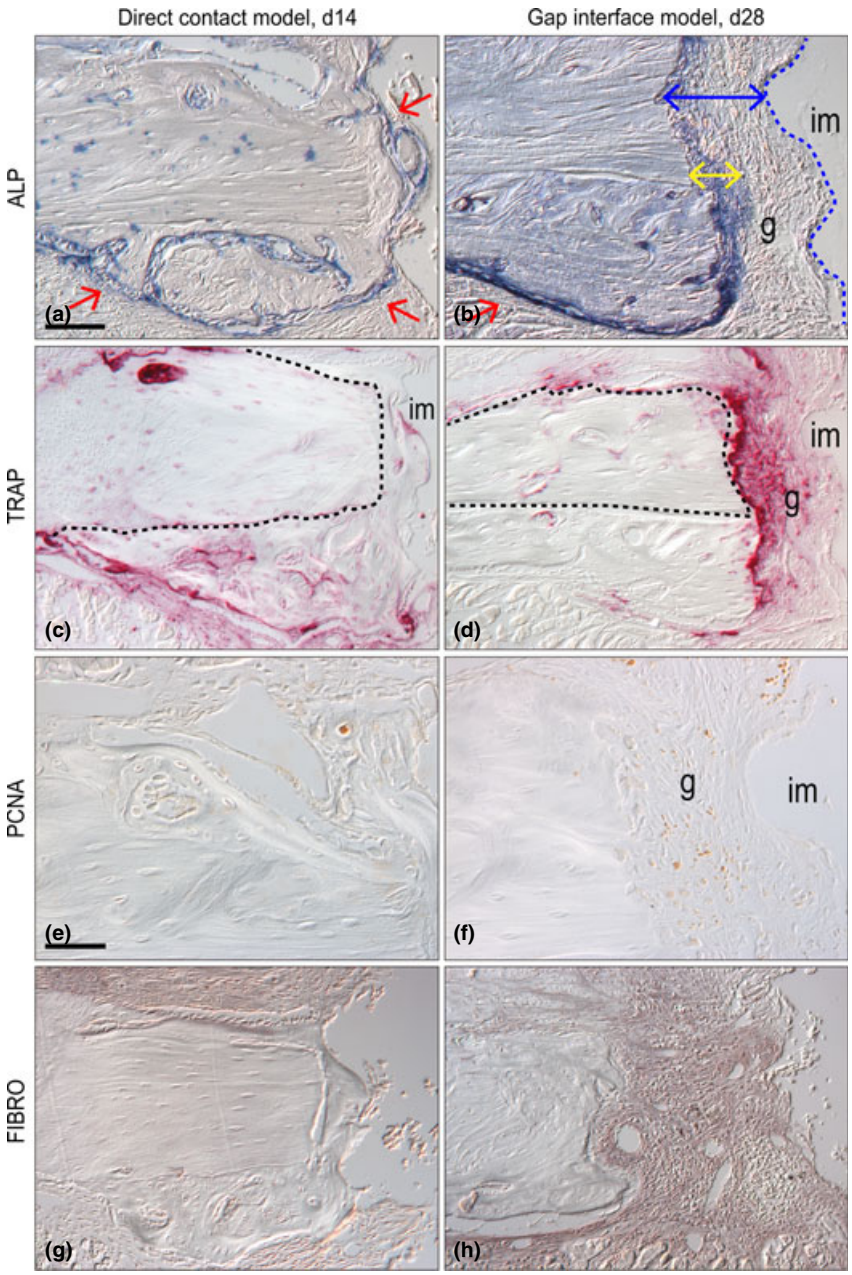

Fig. 3. Molecular differences between osseointegration and fibrous encapsulation. (a) Direct contact implant model on post-surgery day 14, stained with Alkaline phosphatase (ALP) staining, the activity is detectable in the newly mineralizing bone matrix; dotted line indicates native bone, red arrows indicate areas high ALP expression and new bone formation. (b) Gap interface implant model on post-surgery day 28, stained with Alkaline phosphatase staining; yellow double arrow indicates zone of ALP activity, blue double headed arrow indicates area of fibrous tissue, red single arrow indicates new bone formation and dotted blue line indicates implant interface. (c) Representative sagittal tissue section through a direct contact implant on post-surgery day 14, stained with Tartrate resistance acid phosphatase (TRAP) staining. The pink colour denotes the osteoclast activity and dotted line indicates native bone. (d) TRAP staining of gap interface implant model on post-surgery day 28. (e) Direct contact implant model on post-surgery day 14, immunostained for Proliferating Cell Nuclear Antigen (PCNA). (f) PCNA staining of gap interface implant model on post-surgery day 28. (g) Fibromodulin (FIBRO) staining of direct contact implant model on post-surgery day 14. (h) FIBRO staining of gap interface implant model on post-surgery day 28. Scale bars: (a–d; g–h), 100 μm; (e–f) 50 μm.

failed implants? We evaluated TRAP staining as a measure of osteoclast activity (Ashton et al. 1993). In direct contact cases, TRAP activity was tightly restricted to the new bone surfaces adjacent to the implant (Fig. 3c). In implant cases lacking primary stability, TRAP activity was much broader and nearly encompassed the entire peri-implant space including the gap (Fig. 3d).

Cell proliferation continues around failed implants

We found evidence of cell turnover in cases with a gap-interface. Using Proliferating Cell Nuclear Antigen (PCNA) immunostaining to identify cells undergoing active division, we first characterized the control, direct-contact cases, where proliferation was largely constrained to the cells along the edges of the new bone (Fig. 3e). In implants with a gap-interface, cell proliferation was found in the same general region (Fig. 3f), indicating that cell turnover and new bone formation is a ongoing process, even around failed implants. Thus, tissues around an implant lacking primary stability are far from non-viable. Instead, cell proliferation as well as osteogenic differentiation potential and active bone turnover are all active cellular processes found in implant cases characterized by fibrous encapsulation.

A genetic approach to enhancing Wnt signalling prevents implant failure

Given the active state of cell and tissue turnover around implants lacking primary stability, we wondered if the fibroblasts surrounding these failed implants could be converted into matrix-secreting osteoblasts. We approached this question by focusing on the contribution of the pro-osteogenic Wnt signalling pathway to bone formation (Babij et al. 2003, Day et al. 2005, Gaur et al. 2005). To test if Wnt signalling plays a role in osseointegration, we used a strain of Wnt reporter mice, $Axin2^{LacZ/+}$ (Lustig et al. 2002). In the homozygous state (i.e. $Axin2^{LacZ/LacZ}$), mice lack both copies of the negative feedback regulator, Axin2 and consequently, endogenous Wnt signalling is amplified (Minear et al. 2010).

We placed implants in control (wild-type and $Axin2^{LacZ/+}$) and $Axin2^{LacZ/LacZ}$ mice. All implants were placed into a gap-type interface and thus we anticipated that they would all undergo fibrous encapsulation as we had previously documented (Figs 1–3). In wild-type and $Axin2^{LacZ/+}$ mice, this hypothesis was correct : all implants placed into gap-type interfaces showed evidence of fibrous encapsulation of the implant (17/17; see Table 1 and Figs 2 and 3). In sharp contrast, when implants with the same gap-interface were placed into $Axin2^{LacZ/LacZ}$ mice, most underwent osseointegration (9/10; Fig. 4a).

In $Axin2^{LacZ/LacZ}$ peri-implant tissues, Pentachrome and Aniline staining clearly outlined the lamellar architecture of the mature bone (dotted line, Fig. 4a,b) that was distinguished from the woven osteoid matrix occupying the peri-implant space (double headed arrows, Fig. 4a,b). Polarized light and Picrosirius red staining demarcated the native bone (dotted line) from the new osteoid matrix around the implant (arrows, Fig. 4c).

In $Axin2^{LacZ/LacZ}$ mice, ALP activity was evident around the surfaces of the newly forming bone next to the implant and around the blood vessels in the bone (Fig. 4d). In these same samples, TRAP activity was evident on the remodelling surfaces of the new osteoid matrix and

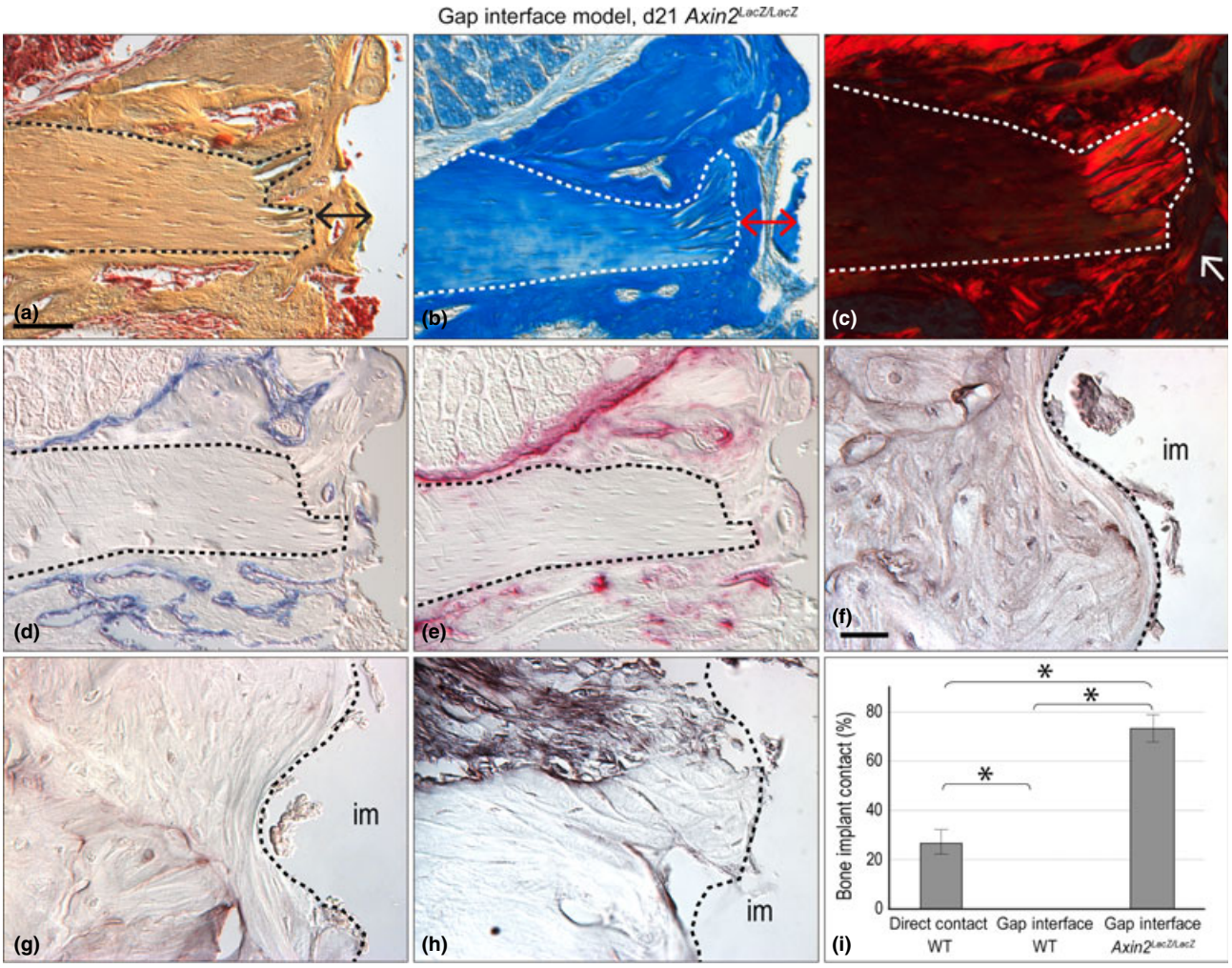

Fig. 4. A genetic approach to enhancing Wnt signalling prevents implant failure. (a) Representative sagittal tissue section through a gap interface model implant on post-surgery day 21 on a $Axin2^{LacZ/LacZ}$ mouse, stained with Pentachrome; dotted line indicates native bone and double headed arrow indicates area of new bone around implant. (b) Aniline blue stain, the dark blue colour denotes collagen in the osteoid tissue, red double headed arrow indicates area of new bone. (c) Picrosirius Red stain, observed with polarized light; the red colour denotes the orientation of the collagen, white arrows indicate organization of new bone. (d) Alkaline phosphatase (ALP) activity is detectable in the newly mineralizing bone matrix. (e) Tartrate resistance acid phosphatase (TRAP) staining, is evident around newly formed bone. (f) Immunostaining for Osteopontin, osteogenic marker. (g) Osteocalcin immunostaining marks osteogenic cells. (h) Decorin immunostaining identifies connective tissue matrix assemblies. (i) The bone-implant contact for three groups were quantified using histomorphometric measurements: group 1 consisted of implants that, when placed, had direct bone contact; group 2 were implants that had a gap-type interface; and group 3, which also had a gap-type interface but were placed in $Axin2^{LacZ/LacZ}$ mice. Scale bars: (a–e), 100 μm; (f–h) 25 μm. Results are presented as the mean ± SEM. * $p \leq 0.05$.

around the lacunae associated with the blood vessels (Fig. 4e). Immunostaining for the pro-osteogenic markers Osteocalcin (Hoffmann et al. 1996) and Osteopontin (Rodan 1995) confirmed that in $Axin2^{LacZ/LacZ}$ mice cells in the gap-type interface were differentiating into osteoblasts (Fig. 4f,g). The $Axin2^{LacZ/LacZ}$ peri-implant tissues was devoid of the fibrous connective tissue marker, Decorin expression (Fig. 4h).

Finally, we used histomorphometry to quantify the amount of peri-implant bone that formed in all of the test cases. Implants that had primary stability at the time of placement had the highest bone-implant contact (BIC) on day 21, in comparison to implants that lacked primary stability at the time of implant placement (Fig. 4i).

We then compared the BIC between $Axin2^{LacZ/LacZ}$ mice with wild-type mice. Recall that in both strains of mice, the implants lacked primary stability at the time of placement. Nonetheless, on day 21 $Axin2^{LacZ/LacZ}$ mice had 70% BIC *versus* 25% BIC in wild-type mice (Fig. 4i). Thus, in cases where primary stability is lacking, elevating the level of endogenous Wnt signalling was sufficient to induce implant osseointegration.

Discussion

The act of cutting into bone, even when using a low-speed drill running at 800 rpm, results in osteocyte cell death. Our data demonstrate empty lacunae evident within 24 h of an osteotomy (Fig. S3, and Mouraret et al. 2013). TUNEL staining of the osteocytes near the cut edge of the alveolar bone indicate that additional osteocytes are undergoing programmed cell death (Mouraret et al. 2013). This cell death triggers a rapid response: osteoclasts immediately begin to resorb the dead bone (Fig. 3) and via the well-described RANKL feedback loop (O'Brien et al. 2013), osteogenesis ensues. Consequently, even in cases where there is direct contact, the alveolar bone resorbs and new bone is deposited. Histologically, the native bone can be distinguished from the new bone by its lamellar architecture (Fig. 3). In cases where direct contact does not exist, the initial cellular responses (i.e. an osteotomy creates a zone of cell death, osteoclasts begin to resorb the mineralized matrix around the empty lacunae, and new bone deposition is initiated) remain the same. The difference, however, is in the extent to which this mineralization occurs: implants lacking primary stability show an abrupt halt in mineralization, falling short of the implant surface (Fig. 3a,b). What factors contribute to this halt in mineralization remain to be determined.

Fibrous encapsulation can arise because of over-loading (Isidor 1996, 1997), a lack of initial primary stability (Fig. 2), or because of an infection around an implant (i.e. peri-implantitis; Jung et al. 2012, Bordin et al. 2009). The principal features that distinguish among these three possible causes of fibrous encapsulation are evidence of initial primary stability and evidence of inflammation and/or infection. In cases of fibrous encapsulation secondary to over-loading, the implant would initially exhibit primary stability, and no evidence of bacterial infection (e.g. suppuration, swelling, redness). In cases of fibrous encapsulation secondary to peri-implantitis, the implant would initially exhibit primary stability, there may also be evidence of new bone formation in contact with the implant surface but this would gradually be lost. In all cases of peri-implantitis, infection is evident early on. Here, we present a model of fibrous encapsulation secondary to the lack of primary stability. At no time-point during the healing phase did we observe bone in contact with the implant surface, or did we observe evidence of infection or inflammation (Fig. S2). By virtue of the model, where the implant bed diameter was larger than the implant itself, implants lack primary stability.

When such irreversible failures of implants occur, clinical standards dictate that the unstable implant must be removed and, if sufficient bone stock remains, replaced. There is little guarantee that the next attempt will be successful largely because the underlying aetiology of the initial failure is oftentimes difficult to ascertain. This is understandable because factors such as the patient's health status and behaviours (Tonetti 1998), conditions of inappropriate loading (Brunski 1999), excessive surgical trauma and infection can all contribute to implant failure (reviewed in Esposito et al. 1998). What if, instead of removal, fibrous encapsulated implants could be induced to osseointegrate?

Defining fibrous encapsulation of an implant

In this study, we relied on histological, cellular and molecular tools, rather than radiographs or physical examinations, to assess the extent of implant osseointegration. We also employed cellular markers of osteogenic differentiation and bone turnover, as well as histological stains, to evaluate the quality and quantity of bone surrounding the implant. Thus, the term "osseointegration" could be rigorously applied to implants placed in direct contact with the maxillary bone (Figs 1, 2a and 3a,c,e).

In wild-type mice, an initial lack of primary stability resulted in fibrous encapsulation as early as day 7, the histological appearance of which did not change over the course of the experiment (Fig. 2). Thus, the presence of fibrous encapsulation around an implant at day 28 represents a persistent state. Furthermore, inflammatory and immunocompetent cells were absent from the fibrous tissue, which is characteristic of late-stage failed implants (Esposito et al. 1997).

Can fibrous encapsulation be reversed?

Despite persist fibrous encapsulation on day 28 we still found evidence of active bone mineralization around failing implants (Fig. 3). The body's attempt at mineralization never culminated in new bone formation, however, apparently because of simultaneous robust osteoclast activity (Fig. 3). Cell turnover, as measured by proliferation markers, indicated the dynamic state of cells in the fibrous sheath but this still did not culminate in bone formation around the implant. These data suggest that cells in a gap-type interface retain the potential to differentiate into osteoblasts, if given the proper physical and/or biological stimuli.

Wnt signalling as an osteogenic stimulus

The Wnt signalling pathway plays a central role in bone development

and homeostasis. In most cases, Wnt ligands promote bone growth (Kim et al. 2007, Leucht et al. 2008b, 2013, Minear et al. 2010), and increase the speed of osseointegration in the tibia (Popelut et al. 2010). We gained insights into the mechanism by which Wnt signalling regulates adult bone repair through the use of the $Axin2^{LacZ/LacZ}$ mouse strain, in which the cellular response to Wnt signalling is increased because of the removal of a negative Wnt regulator (Minear et al. 2010). Unlike wild-type littermates, implants with a gap-interface undergo osseointegration in $Axin2^{LacZ/LacZ}$ mice (Fig. 4).

We did not observe fibrous encapsulation of implants placed in $Axin2^{LacZ/LacZ}$ mice. Even though there was no initial primary stability (a state which dictates that the maxillary implant will fail in wild-type mice), bone formed in the gap-type interface created in $Axin2^{LacZ/LacZ}$ mice (Fig. 4). From these data, we conclude that primary stability is not a prerequisite for implant osseointegration. At least in this model system, elevated Wnt signalling can overcome the disadvantages resulting from a lack of primary stability. Elevated Wnt signalling, as seen in $Axin2^{LacZ/LacZ}$ mice, prevented implant failure. This finding suggests that delivery of a pro-osteogenic stimulus around an implant may improve the chances of osseointegration especially in those cases where anatomy or previous disease has compromised the implant bed.

References

Albrektsson, T., Zarb, G., Worthington, P. & Eriksson, A. R. (1986) The long-term efficacy of currently used dental implants: a review and proposed criteria of success. *International Journal of Oral and Maxillofacial Implants* **1**, 11–25.

Ashton, B. A., Ashton, I. K., Marshall, M. J. & Butler, R. C. (1993) Localisation of vitronectin receptor immunoreactivity and tartrate resistant acid phosphatase activity in synovium from patients with inflammatory or degenerative arthritis. *Annals of the Rheumatic Diseases* **52**, 133–137.

Babij, P., Zhao, W., Small, C., Kharode, Y., Yaworsky, P. J., Bouxsein, M. L., Reddy, P. S., Bodine, P. V., Robinson, J. A., Bhat, B., Marzolf, J., Moran, R. A. & Bex, F. (2003) High bone mass in mice expressing a mutant LRP5 gene. *Journal of Bone and Mineral Research* **18**, 960–974.

Bordin, S., Flemmig, T. F. & Verardi, S. (2009) Role of fibroblast populations in peri-implantitis. *International Journal of Oral and Maxillofacial Implants* **24**, 197–204.

Branemark, P. I., Hansson, B. O., Adell, R., Breine, U., Lindstrom, J., Hallen, O. & Ohman, A. (1977) Osseointegrated implants in the treatment of the edentulous jaw: experience from a 10-year period. *Scandinavian Journal of Plastic and Reconstructive Surgery. Supplementum* **16**, 1–132.

Brunski, J. B. (1999) *In vivo* bone response to biomechanical loading at the bone/dental-implant interface. *Advances in Dental Research* **13**, 99–119.

Day, T. F., Guo, X., Garrett-Beal, L. & Yang, Y. (2005) Wnt/beta-catenin signaling in mesenchymal progenitors controls osteoblast and chondrocyte differentiation during vertebrate skeletogenesis. *Developmental Cell* **8**, 739–750.

Dayan, D., Hiss, Y., Hirshberg, A., Bubis, J. J. & Wolman, M. (1989) Are the polarization colors of picrosirius red-stained collagen determined only by the diameter of the fibers? *Histochemistry* **93**, 27–29.

Esposito, M., Hirsch, J. M., Lekholm, U. & Thomsen, P. (1998) Biological factors contributing to failures of osseointegrated oral implants. (II) Etiopathogenesis. *European Journal of Oral Sciences* **106**, 721–764.

Esposito, M., Thomsen, P., Molne, J., Gretzer, C., Ericson, L. E. & Lekholm, U. (1997) Immunohistochemistry of soft tissues surrounding late failures of Branemark implants. *Clinical Oral Implants Research* **8**, 352–366.

Gaur, T., Lengner, C. J., Hovhannisyan, H., Bhat, R. A., Bodine, P. V., Komm, B. S., Javed, A., van Wijnen, A. J., Stein, J. L., Stein, G. S. & Lian, J. B. (2005) Canonical WNT signaling promotes osteogenesis by directly stimulating Runx2 gene expression. *Journal of Biological Chemistry* **280**, 33132–33140.

Hoffmann, H. M., Beumer, T. L., Rahman, S., McCabe, L. R., Banerjee, C., Aslam, F., Tiro, J. A., van Wijnen, A. J., Stein, J. L., Stein, G. S. & Lian, J. B. (1996) Bone tissue-specific transcription of the osteocalcin gene: role of an activator osteoblast-specific complex and suppressor hox proteins that bind the OC box. *Journal of Cellular Biochemistry* **61**, 310–324.

Huwiler, M. A., Pjetursson, B. E., Bosshardt, D. D., Salvi, G. E. & Lang, N. P. (2007) Resonance frequency analysis in relation to jawbone characteristics and during early healing of implant installation. *Clinical Oral Implants Research* **18**, 275–280.

Isidor, F. (1996) Loss of osseointegration caused by occlusal load of oral implants. A clinical and radiographic study in monkeys. *Clinical Oral Implants Research* **7**, 143–152.

Isidor, F. (1997) Histological evaluation of peri-implant bone at implants subjected to occlusal overload or plaque accumulation. *Clinical Oral Implants Research* **8**, 1–9.

Jung, S. R., Bashutski, J. D., Jandali, R., Prasad, H., Rohrer, M. & Wang, H. L. (2012) Histological analysis of soft and hard tissues in a periimplantitis lesion: a human case report. *Implant Dentistry* **21**, 186–189.

Kim, J. B., Leucht, P., Lam, K., Luppen, C., Ten Berge, D., Nusse, R. & Helms, J. A. (2007) Bone regeneration is regulated by wnt signaling. *Journal of Bone and Mineral Research* **22**, 1913–1923.

Leucht, P., Jiang, J., Cheng, D., Liu, B., Dhamdhere, G., Fang, M. Y., Monica, S. D., Urena, J. J., Cole, W., Smith, L. R., Castillo, A. B., Longaker, M. T. & Helms, J. A. (2013) Wnt3a reestablishes osteogenic capacity to bone grafts from aged animals. *Journal of Bone and Joint Surgery. American Volume* **95**, 1278–1288.

Leucht, P., Kim, J. B., Amasha, R., James, A. W., Girod, S. & Helms, J. A. (2008a) Embryonic origin and Hox status determine progenitor cell fate during adult bone regeneration. *Development (Cambridge, England)* **135**, 2845–2854.

Leucht, P., Kim, J. B. & Helms, J. A. (2008b) Beta-catenin-dependent Wnt signaling in mandibular bone regeneration. *Journal of Bone and Joint Surgery. American Volume* **90** (Suppl 1), 3–8.

Leucht, P., Kim, J. B., Wazen, R., Currey, J. A., Nanci, A., Brunski, J. B. & Helms, J. A. (2007) Effect of mechanical stimuli on skeletal regeneration around implants. *Bone* **40**, 919–930.

Leucht, P., Monica, S. D., Temiyasathit, S., Lenton, K., Manu, A., Longaker, M. T., Jacobs, C. R., Spilker, R. L., Guo, H., Brunski, J. B. & Helms, J. A. (2012) Primary cilia act as mechanosensors during bone healing around an implant. *Medical Engineering & Physics* **35**, 392–402.

Liu, B., Hunter, D. J., Rooker, S., Chan, A., Paulus, Y. M., Leucht, P., Nusse, Y., Nomoto, H. & Helms, J. A. (2013) Wnt signaling promotes Muller cell proliferation and survival after injury. *Investigative Ophthalmology & Visual Science* **54**, 444–453.

Lustig, B., Jerchow, B., Sachs, M., Weiler, S., Pietsch, T., Karsten, U., van de Wetering, M., Clevers, H., Schlag, P. M., Birchmeier, W. & Behrens, J. (2002) Negative feedback loop of Wnt signaling through upregulation of conductin/Axin2 in colorectal and liver tumors. *Molecular and Cellular Biology* **22**, 1184–1193.

Meredith, N. (1998) Assessment of implant stability as a prognostic determinant. *The International Journal of Prosthodontics* **11**, 491–501.

Meredith, N., Alleyne, D. & Cawley, P. (1996) Quantitative determination of the stability of the implant-tissue interface using resonance frequency analysis. *Clinical Oral Implants Research* **7**, 261–267.

Minear, S., Leucht, P., Jiang, J., Liu, B., Zeng, A., Fuerer, C., Nusse, R. & Helms, J. A. (2010) Wnt proteins promote bone regeneration. *Science Translational Medicine* **2**, 29ra30.

Mouraret, S., Hunter, D. J., Bardet, C., Brunski, J. B., Bouchard, P. & Helms, J. A. (2013) A pre-clinical murine model of oral implant osseointegration. *Bone*, doi:10.1016/j.bone.2013.07.021.

O'Brien, C. A., Nakashima, T. & Takayanagi, H. (2013) Osteocyte control of osteoclastogenesis. *Bone* **54**, 258–263.

Pjetursson, B. E., Thoma, D., Jung, R., Zwahlen, M. & Zembic, A. (2012) A systematic review of the survival and complication rates of implant-supported fixed dental prostheses (FDPs) after a mean observation period of at least 5 years. *Clinical Oral Implants Research* **23** (Suppl 6), 22–38.

Popelut, A., Rooker, S. M., Leucht, P., Medio, M., Brunski, J. B. & Helms, J. A. (2010) The acceleration of implant osseointegration by liposomal Wnt3a. *Biomaterials* **31**, 9173–9181.

Raghavendra, S., Wood, M. C. & Taylor, T. D. (2005) Early wound healing around endosseous implants: a review of the literature. *International Journal of Oral and Maxillofacial Implants* **20**, 425–431.

Richardson, M. (2009) A developmental biologist highlights potential pitfalls of using stem cells that can "remember" their origins [WWW document].

Rodan, G. A. (1995) Osteopontin overview. *Annals of the New York Academy of Sciences* **760**, 1–5.
Stucki, U., Schmid, J., Hammerle, C. F. & Lang, N. P. (2001) Temporal and local appearance of alkaline phosphatase activity in early stages of guided bone regeneration. A descriptive histochemical study in humans. *Clinical Oral Implants Research* **12**, 121–127.
Tonetti, M. S. (1998) Risk factors for osseodisintegration. *Periodontology 2000* **17**, 55–62.
Wazen, R. M., Currey, J. A., Guo, H., Brunski, J. B., Helms, J. A. & Nanci, A. (2013) Micromotion-induced strain fields influence early stages of repair at bone-implant interfaces. *Acta Biomaterialia* **24**, 313–324.
Weis, S. M., Zimmerman, S. D., Shah, M., Covell, J. W., Omens, J. H., Ross, J. Jr, Dalton, N., Jones, Y., Reed, C. C., Iozzo, R. V. & McCulloch, A. D. (2005) A role for decorin in the remodeling of myocardial infarction. *Matrix Biology* **24**, 313–324.

Supporting Information

Additional Supporting Information may be found in the online version of this article:

Figure S1. An failure implant model in mice. (a) Pre-operative photograph of the alveolar crest, anterior to the maxillary first molar; black-dotted line indicates incision placement. (b) The intrasulcular incision extends from the lingual surface of the maxillary first molar anteriorly, to the crest of the edentulous space. (c) A full-thickness flap is elevated to expose the alveolar bone. (d) A 0.65 mm hole is prepared on the crest, 1.5 mm anterior of the first maxillary molar. (e) The 0.6 mm diameter titanium alloy implant. (f) The implant is placed manually, followed by careful rinsing. (g) Wounds are closed with non-absorbable single interrupted sutures. (h) Skeletal preparation showing location of the maxillary implant relative to the dentition and bones of the skull. (i) Soft tissue covered the healing implant days post-surgery. M1, maxilla first molar; ab, alveolar bone. Scale bars: (a–d, f–i) 900 μm; (e) 2500 μm; (h) 1500 μm.

Figure S2. Analysis of the Osteotomy. (a) Representative sagittal tissue section through a maxilla cut bone site using a low-speed drill running at 800 rpm, post-surgery day 1, cut site indicated by white rectangle. (b) Stained with DAPI; blue indicates cell nuclei and empty lacunae were detected within 24 h of the osteotomy. (c) TUNEL staining, observed with fluorescent light, the green colour denotes cells undergoing apoptosis near the cut site. (d) TRAP staining is evident around cut bone indicate osteocytes near the cut. Scale bars: (a–e), 100 μm.

Figure S3. Inflammation of the Implant. (a) Direct contact implant model on post-surgery day 7, stained with GR1 antibody, indicates granulocytes and peripheral neutrophils. (b) Representative sagittal tissue section, stained with GR1, through a gap interface model implant on post-surgery day 7. Scale bars: (a–b), 100 μm.

Address:
Jill A. Helms
257 Campus Drive
PSRL Building
Stanford
CA 94305
USA
E-mail: jhelms@stanford.edu

Clinical Relevance

Scientific rationale for the study: Implants can fail, but discriminating between the ones that are destined to fail and those that will ultimately succeed can be difficult. This represents a real and ongoing challenge to clinicians, who are oftentimes forced to place implants into patients with pre-disposing factors, or in oral sites where sufficient bony support is unavailable.
Principal findings: We created a mouse model of implant failure by ensuring that the implant lacked primary stability. The characteristics of this model closely mirror what is observed in large animal models and in humans, but has a distinct advantage: a wide array of molecular, cellular and genetic tools can be used to characterize the process of fibrous encapsulation. Our study revealed that even in a fibrous capsule surrounding a loose implant, there is still evidence of cell proliferation and active bone turnover. We showed that fibrous encapsulation could be prevented, even in cases where there is no primary stability, by modulating a stem cell growth factor that is responsible for bone induction.
Practical implications: This mouse model can be used to test the influence of implant surface modifications, time to loading, and biological stimuli on the ability to reverse or prevent implant instability, which may then inform the clinical practice of implantology in humans.